fractal and fractional

MDPI

Article

Asymptotic and Pinning Synchronization of Fractional-Order Nonidentical Complex Dynamical Networks with Uncertain Parameters

Yu Wang, Xiliang He * and Tianzeng Li

School of Mathematics and Statistics, Sichuan University of Science and Engineering, Zigong 643000, China; jdwangyu@suse.edu.cn (Y.W.); litianzeng@suse.edu.cn (T.L.)
* Correspondence: 321070108109@stu.suse.edu.cn

Abstract: This paper is concerned with the asymptotic and pinning synchronization of fractional-order nonidentical complex dynamical networks with uncertain parameters (FONCDNUP). First of all, some synchronization criteria of FONCDNUP are proposed by using the stability of fractional-order dynamical systems and inequality theory. Moreover, a novel controller is derived by using the Lyapunov direct method and the differential inclusion theory. Next, based on the Lyapunov stability theory and pinning control techniques, a new group of sufficient conditions to assure the synchronization for FONCDNUP are obtained by adding controllers to the sub-nodes of networks. At last, two numerical simulations are utilized to illustrate the validity and rationality of the acquired results.

Keywords: pinning synchronization; nonidentical networks; uncertain parameters

Citation: Wang, Y.; He, X.; Li, T. Asymptotic and Pinning Synchronization of Fractional-Order Nonidentical Complex Dynamical Networks with Uncertain Parameters. *Fractal Fract.* **2023**, *7*, 571. https://doi.org/10.3390/fractalfract7080571

Academic Editors: Gani Stamov, Libo Feng, Lin Liu and Yang Liu

Received: 20 May 2023
Revised: 23 July 2023
Accepted: 23 July 2023
Published: 25 July 2023

1. Introduction

As is known to all, complex networks cover almost everywhere and have been rapidly growing with a wide range of applications. Over the past few decades, several results on the dynamical behavior of complex dynamical networks have been published, such as chaos [1], bifurcation [2], stability [3], and dissipativity [4].

Fractional-order derivatives, as a generalization of integer-order derivatives, can describe natural phenomena more easily. Moreover, fractional-order derivatives have more advantages than integer-order derivatives in terms of memory and genetic properties. Additionally, they have a wide range of promising applications in secure communications [5], viscoelastic systems [6], power systems [7], robotics [8], and heat conduction [9]. Furthermore, real-world models can be better portrayed by fractional-order derivatives, such as hydrodynamics [10] and biological models [11]. It is necessary to introduce fractional-order derivatives in complex networks. Additionally, fractional-order complex networks (FOCN) can be seen as an important stretch of traditional integer-order complex networks, which have excellent modeling capabilities and are well suited to assist people in physics, engineering, and interdisciplinary areas to simulate a variety of materials and systems with longtime memory and genetic properties [12–14]. It is worth noting that dynamical characteristics such as the synchronization of FOCN occupy an important position in applications and are gradually gaining attention. Therefore, theoretical and applied studies of FOCN are very important and interesting [15].

Dynamical phenomena in complex networks have been broadly studied, among which the synchronization is one of the most critical dynamic activities in complex networks. In reality, synchronization as a kind of basic natural activity has been extensively studied in different fields. The synchronization of FOCN as an interesting and essential dynamical behavior has been studied by a large amount of scholars and has a wide range of research in unmanned ground vehicles [16], cryptography [17], and image encryption [18]. Hence, there has been a great deal of research on synchronization [19,20]. The synchronization of

FOCN by specific control strategies is an increasingly important issue in control of FOCN. Many strategies have been proposed for synchronous control [21,22], and they are widely applied in different areas. However, because the FOCN is made up of many nodes, these effective control strategies are difficult and costly to implement as they require moment by moment control of the entire node. They require constant activation of control inputs, which can result in wasted energy. Therefore, pinning control is no doubt a more efficient control method because pinning control synchronizes the network by controlling a small portion of the nodes instead of all of them [23].

Most of the models studied in the current works have the same parameters. However, due to the complexity of the real world, the parameters of the drive and response systems are hardly identical. Therefore, considering that, a nonidentical network with different parameters for the driving system and the response system is more realistic [24].

In reality, the presence of parameter uncertainty is inevitable. This is why we cannot always obtain the precise values of the parameters used in modeling the real system. Additionally, there may be unknown topology and modeling errors. Uncertain parameters can result in the negative dynamic behavior of the system, such as decreased performance, prolonged synchronization time, and even the destabilization of the trajectory. Therefore, it is important to consider the effects of parameter uncertainty on the system. Incorporating parameter uncertainty into the network model is essential.

For instance [25], the authors utilized the comparison theorem and Lyapunov method to derive conditions for the synchronization of the FOCN with multiple time delays and parameter uncertainty. Additionally, in the literature [26], they employed the homogeneous embryonic principle and inequality techniques to establish two criteria—one independent of time delay and one dependent on time delay—in order to ensure the accuracy of the conclusions. Apart from that, in [27], the authors obtained conditions for achieving projection synchronization by modeling fractional-order T-S fuzzy neural networks with uncertain parameters and applying system stability theory and matrix inequality techniques. In the [28], a new sliding-mode surface controller on nonidentical networks was designed. In Ref. [29], some sufficient conditions were derived to achieve the synchronization of the global Mittag–Leffler projection of the processing model using the Lyapunov method and the Razumikhin technique to converge the states to a specified sliding surface for sliding motion. In Ref. [30], the synchronization of the FOCN with delays under adaptive control was achieved using inequality theory and the comparison principle of linear fractional equations with delays. In order to achieve asymptotic synchronization of uncertain FOCN, an adaptive pinning controller was designed in the paper [31]. In Ref. [32], it was demonstrated that the uncertain fractional-order T-S fuzzy complex networks were stable under the designed controller, reducing the impact of coupled time-varying and uncertainty perturbations on the tracking error. However, there is a scarcity of relevant studies on the pinning synchronization of FOCN with parameter uncertainty, making it a worthwhile area for exploration.

Motivated by the above discussions, this paper mainly considers the asymptotic and pinning synchronization of FONCDNUP. The main contributions are as follows:

(1) By employing stability and the inequality theory of fractional dynamical systems, a new criterion for the synchronization of FONCDNUP is discovered.

(2) By utilizing the Lyapunov direct method and pinning control theory, a novel pinning controller is designed.

(3) Since there is limited research on pinning control in FOCN with parameter uncertainty, the previous studies are extended.

The remainder of the paper is organized as follows: Section 2 provides the preliminaries; Section 3 presents some sufficient conditions for the asymptotic and pinning synchronization of FOCN with uncertain parameters; the effectiveness of the obtained results is verified through simulations in Section 4; and finally, Section 5 concludes the paper and offers prospects for future research.

2. Preliminaries

Definition 1 ([33]). *The function $\tilde{\hbar}(t)$ with α-order fractional integral is defined as*

$$I_t^{\alpha}\tilde{\hbar}(t) = \frac{1}{\Gamma(\alpha)}\int_{t_0}^{t}(t-s)^{\alpha-1}\tilde{\hbar}(s)ds, \tag{1}$$

where $\alpha > 0$, t_0 is the initial time, and $t \geq t_0$, $\Gamma(\cdot)$ is the Euler gamma function.

Definition 2 ([33]). *The function $\tilde{\hbar}(t)$ with α-order Caputo derivative of fractional is defined as follows:*

$${}_{t_0}^{C}D_t^{\alpha}\tilde{\hbar}(t) = \frac{1}{\Gamma(\hat{k}-\alpha)}\int_{t_0}^{t}(t-v)^{\hat{k}-\alpha-1}\tilde{\hbar}(t)^{(\hat{k})}(v)dv, \tag{2}$$

where $\hat{k}-1 < \alpha < \hat{k}$, $\hat{k} \in \mathbb{Z}^+$, and t_0 is the initial time. And in particular, when $0 < \alpha < 1$,

$${}_{t_0}^{C}D_t^{\alpha}\tilde{\hbar}(t) = \frac{1}{\Gamma(1-\alpha)}\int_{t_0}^{t}(t-v)^{-\alpha}\tilde{\hbar}'(t)(v)dv. \tag{3}$$

Lemma 1 ([34]). *For all $0 < \alpha < 1$, if $\tilde{\hbar}(t) \in C^1([t,+\infty),\mathbb{R})$, then*

$${}_{t_0}^{C}D_t^{\alpha}|\tilde{\hbar}(t)| \leq \operatorname{sign}(\tilde{\hbar}(t)){}_{t_0}^{C}D_t^{\alpha}\tilde{\hbar}(t), \tag{4}$$

where $t \geq t_0$, and t_0 is the initial time.

Lemma 2 ([35]). *$P \in \mathbb{R}^{n\times n}$ is a positive-definite matrix, and $\forall$ vectors ϖ, $s \in \mathbb{R}^n$, the below inequality holds true:*

$$\varpi^{\top}s \leq \frac{1}{2}\varpi^{\top}P\varpi + \frac{1}{2}s^{\top}P^{-1}s. \tag{5}$$

Assumption 1. *The activation functions $\tilde{\hbar}_i(\cdot)$; for all $i = 1,2,\cdots,n$, it satisfies the Lipschitz conditions if a positive matrix $L = diag(l_1,l_2,\cdots,l_n)$ exists such that*

$$|\tilde{\hbar}_i(t,s) - \tilde{\hbar}_p(t,\varpi)| \leq L_i|s-\varpi|, \tag{6}$$

for all $\varpi, s \in \mathbb{R}^n$.

3. Main Results

In this section, one can obtain some results on asymptotic and pinning synchronization of FOCN with uncertain parameters by means of Lyapunov theory and inequality theory, and some controllers are designed to ensure that synchronization is realizable.

3.1. Asymptotic Synchronization for FONCDNUP

In this segment, the work synchronizes the system (7) and system (8) by an appropriate controller. Then, one will consider the below FONCDNUP: the drive system is described as

$${}_{t_0}^{c}D_t^{\alpha}\varpi_i(t) = A_0\varpi_i(t) + B_0\hbar(\varpi_i(t)) + c\sum_{j=1}^{N}d_{ij}\Lambda\varpi_j(t), \tag{7}$$

and the response system is described as

$${}_{t_0}^{c}D_t^{\alpha}s_i(t) = (E_0+\Delta E(t))s_i(t) + (G_0+\Delta G(t))\hbar(s_i(t)) + c\sum_{j=1}^{N}d_{ij}\Lambda s_j(t) + u_i(t), \tag{8}$$

where $0 < \alpha < 1$, $i = 1,2,\cdots,n$; $\varpi_i(t)$ and $s_i(t)$ are the state of the i-node, A_0 and E_0 are constant matrices, $\hbar(\varpi_i(t))$, and $\hbar(s_i(t))$ indicate the continuous nonlinear functions. B_0 and G_0 stand for the weight matrices. $\Lambda = \operatorname{diag}(\varepsilon_1,\varepsilon_2,\cdots,\varepsilon_n) > 0$ is the internal coupling matrix. $(d_{ij})_{n\times n}$ is the outer coupling matrix, and if it has a linkage in the node i to j, $d_{ij} \neq 0$; otherwise $d_{ij} = 0$. $\Delta E(t)$ and $\Delta G(t)$ are the parametric uncertainties.

The vector of synchronization error (sync-error) is defined as

$$e_i(t) = s_i(t) - \varpi_i(t). \tag{9}$$

Based on (7) and (8), the sync-error system is as follows:

$$\begin{aligned} {}_{t_0}^{c}D_t^{\alpha} e_i(t) =& {}_{t_0}^{c}D_t^{\alpha} s_i(t) - {}_{t_0}^{c}D_t^{\alpha} \varpi_i(t) \\ =& (E_0 + \Delta E(t)) s_i(t) + (G_0 + \Delta G(t)) \hbar(s_i(t)) \\ & - B_0 \hbar(\varpi_i(t)) - A_0 \varpi_i(t) + c \sum_{j=1}^{N} d_{ij} \Lambda e_i(t) + u_i(t), \end{aligned} \tag{10}$$

where $i = 1, 2, \cdots, n$.

In order to obtain the main results, one makes the following assumption.

Assumption 2. *The parametric uncertainties $\Delta E(t)$, $\Delta G(t)$, $\Delta D(t)$, and $\Delta Q(t)$ are the following forms:*

$$\begin{aligned} \Delta E(t) &= M_e F(t) H_e, \\ \Delta G(t) &= M_g F(t) H_g, \\ \Delta D(t) &= M_d F(t) H_d, \\ \Delta Q(t) &= M_q F(t) H_q, \end{aligned}$$

where M_e, M_g, H_e, H_g, H_d, H_q, M_d, and M_q are the diagonal matrices with appropriate dimensions. And the uncertain matrix $F(t)$ can satisfy $F^{\top}(t)F(t) \leq I$, where I is the identity matrix.

Theorem 1. *Under the Assumptions 1 and 2, and scalar $0 < \alpha < 1$, FONCDNUP can achieve asymptotic synchronization, if the following inequalities hold:*

(i) $\hat{\Upsilon} < 0$,

(ii) $u_i(t) = -(E_0 + \Delta E(t) - A_0)\varpi_i(t) - (G_0 + \Delta G(t))\hbar(\varpi_i(t)) + B_0 \hbar(\varpi_i(t) - \delta_i e_i(t)$,

and $\hat{\Upsilon} = E_0 + \frac{1}{2} M_e M_e^{\top} + \frac{1}{2} H_e^{\top} H_e + L G_0 + L \frac{1}{2} M_g M_g^{\top} + L \frac{1}{2} H_g^{\top} H_g + \sum_{j=1}^{N} d_{ij} \Lambda - \delta_i$.

Proof. Construct the following Lyapunov function:

$$V(t) = \sum_{i=1}^{n} |e_i(t)|, \tag{11}$$

then, taking the fractional derivative of $V(t)$ by Lemma 1, we can obtain

$$\begin{aligned} {}_{t_0}^{c}D_t^{\alpha} V(t) =& {}_{t_0}^{c}D_t^{\alpha} \sum_{i=1}^{n} |e_i(t)| \\ \leq & \sum_{i=1}^{n} \operatorname{sign}^{\top}(e_i(t)) {}_{t_0}^{c}D_t^{\alpha} e_i(t) \\ \leq & \sum_{i=1}^{n} \operatorname{sign}^{\top}(e_i(t)) [(E_0 + \Delta E(t)) s_i(t) - A_0 \varpi_i(t) - B_0 \hbar(\varpi_i(t)) \\ & + (G_0 + \Delta G(t)) \hbar(s_i(t) + c \sum_{j=1}^{N} d_{ij} \Lambda e_i(t) + u_i(t)] \\ \leq & \sum_{i=1}^{n} \operatorname{sign}^{\top}(e_i(t)) [(E_0 + \Delta E(t)) s_i(t) - A_0 \varpi_i(t)] \\ & + \sum_{i=1}^{n} \operatorname{sign}^{\top}(e_i(t) [(G_0 + \Delta G(t)) \hbar(s_i(t)) - B_0 \hbar(\varpi_i(t))] \\ & + \sum_{i=1}^{n} \operatorname{sign}^{\top}(e_i(t)) c \sum_{j=1}^{N} d_{ij} \Lambda e_i(t) + \sum_{i=1}^{n} sign^{\top}(e_i(t)) u_i(t). \end{aligned} \tag{12}$$

It follows from Lemma 2 and Assumption 2 that

$$\begin{aligned} W_1 &= \sum_{i=1}^{n} \operatorname{sign}^{\top}(e_i(t)(E_0+\Delta E(t))s_i(t) - A_0\varpi_i(t) \\ &\le \sum_{F=1}^{n} |(E_0+\Delta E(t))s_i(t) + (E_0+\Delta E(t)))\varpi_i(t) \\ &\quad - (E_0+\Delta E(t))\varpi_i(t) - A_0\varpi_i(t)| \\ &\le \sum_{i=1}^{n} |(E_0+\Delta E(t))e_i(t) + (E_0 - A_0 + \Delta E(t))\varpi_i(t)| \\ &\le \sum_{i=1}^{n} |(E_0+M_eF(t)H_e)e_i(t) + (E_0+M_eF(t)H_e - A_0)\varpi_i(t)| \\ &\le \sum_{i=1}^{n} |(E_0+\frac{1}{2}M_eM_e^{\top} + \frac{1}{2}H_e^{\top}H_e)e_i(t) \\ &\quad + (E_0+\frac{1}{2}M_eM_e^{\top} + \frac{1}{2}H_e^{\top}H_e - A_0)\varpi_i(t)|. \end{aligned} \tag{13}$$

Using Assumption 1, one has

$$\begin{aligned} W_2 &= \sum_{i=1}^{n} \operatorname{sign}^{\top}(e_i(t)[(G_0+\Delta G(t))\hbar(s_i(t)) - B_0\hbar(\varpi_i(t))] \\ &\le \sum_{i=1}^{n} |(G_0+\Delta G(t))\hbar(s_i(t)) - B_0\hbar(\varpi_i(t))| \\ &\le \sum_{i=1}^{n} (G_0+\Delta G(t))\hbar(s_i(t)) + (G_0+\Delta G(t))\hbar(\varpi_i(t) \\ &\quad - (G_0+\Delta G(t))\hbar(\varpi_i(t)) - B_0\hbar(\varpi_i(t) \\ &\le \sum_{i=1}^{n} |(G_0+\Delta G(t))Le_i(t) + (G_0+\Delta G(t))\hbar(\varpi_i(t)) - B_0\hbar(\varpi_i(t)) \\ &\le \sum_{i=1}^{n} |(G_0+M_gF(t)H_g)Le_i(t) + (G_0+M_gF(t)H_g)\hbar(\varpi_i(t)) - B_0\hbar(\varpi_i(t) \\ &\le \sum_{i=1}^{n} |(G_0+\frac{1}{2}M_gM_g^{\top} + \frac{1}{2}H_g^{\top}H_g)Le_i(t) - B_0\hbar(\varpi_i(t) \\ &\quad + (G_0+\frac{1}{2}M_gM_g^{\top} + \frac{1}{2}H_g^{\top}H_g)\hbar(\varpi_i(t))|. \end{aligned} \tag{14}$$

Similarly, one can obtain the following formula:

$$\begin{aligned} W_3 &= \sum_{i=1}^{n} \operatorname{sign}^{\top}(e_i(t))c\sum_{j=1}^{N} d_{ij}\Lambda e_i(t) \\ &\le \sum_{i=1}^{n} |c\sum_{j=1}^{N} d_{ij}\Lambda e_i(t)| \\ &\le c\sum_{i=1}^{n}\sum_{j=1}^{N} d_{ij}\Lambda|e_i(t)|. \end{aligned} \tag{15}$$

Adding the controller $u_i(t)$ to (12), we obtain

$$\begin{aligned} W_4 &= \sum_{i=1}^{n} \operatorname{sign}^{\top}(e_i(t))u_i(t) \\ &\leq \sum_{i=1}^{n} \operatorname{sign}^{\top}(e_i(t))[-(E_0+\Delta E(t)-A_0)\varpi_i(t)-\delta_i e_i(t) \\ &\quad -(G_0+\Delta G(t))\hbar(\varpi_i(t))+B_0\hbar(\varpi_i(t)] \\ &\leq \sum_{i=1}^{n} |-(E_0+\Delta E(t)-A_0)\varpi_i(t)-\delta_i e_i(t) \\ &\quad -(G_0+\Delta G(t))\hbar(\varpi_i(t))+B_0\hbar(\varpi_i(t)| \\ &\leq \sum_{i=1}^{n} |-(E_0+\frac{1}{2}M_eM_e^{\top}+\frac{1}{2}H_e^{\top}H_e)\varpi_i(t)+B_0\hbar(\varpi_i(t) \\ &\quad -(G_0+\frac{1}{2}M_gM_g^{\top}+\frac{1}{2}H_g^{\top}H_g)\hbar(\varpi_i(t))-\delta_i e_i(t)+A_0\varpi_i(t)|. \end{aligned} \tag{16}$$

By adding (13)–(16) to (12), one can obtain

$$\begin{aligned} {}_{t_0}^{c}D_t^{\alpha}V(t) \leq & W_1+W_2+W_3+W_4 \\ \leq & \sum_{i=1}^{n} |(E_0+\frac{1}{2}M_eM_e^{\top}+\frac{1}{2}H_e^{\top}H_e)e_i(t)E_0\varpi_i(t)-A_0\varpi_i(t) \\ & +(\frac{1}{2}M_eM_e^{\top}+\frac{1}{2}H_e^{\top}H_e)\varpi_i(t)+\frac{1}{2}M_gM_g^{\top}Le_i(t) \\ & +G_0Le_i(t)+\frac{1}{2}H_g^{\top}H_gLe_i(t)+\frac{1}{2}H_g^{\top}H_g\hbar(\varpi_i(t)) \\ & +(G_0+\frac{1}{2}M_gM_g^{\top})\hbar(\varpi_i(t))-B_0\hbar(\varpi_i(t))+A_0\varpi_i(t) \\ & -(E_0+\frac{1}{2}M_eM_e^{\top}+\frac{1}{2}H_e^{\top}H_e)\varpi_i(t)+\sum_{j=1}^{N}d_{ij}\Lambda e_i(t) \\ & -(G_0+\frac{1}{2}M_gM_g^{\top}+\frac{1}{2}H_g^{\top}H_g)\hbar(\varpi_i(t))-\delta_i e_i(t)+B_0\hbar(\varpi_i(t)| \\ \leq & \sum_{i=1}^{n}[E_0+\frac{1}{2}M_eM_e^{\top}+\frac{1}{2}H_e^{\top}H_e+LG_0+L\frac{1}{2}M_gM_g^{\top} \\ & +L\frac{1}{2}H_g^{\top}H_g+\sum_{j=1}^{N}d_{ij}\Lambda-\delta_i]|e_i(t)| \\ \leq & \sum_{i=1}^{n}\hat{\Upsilon}|e_i(t)|. \end{aligned} \tag{17}$$

When $\hat{\Upsilon}<0$, the ${}_{t_0}^{c}D_t^{\alpha}V(t)\leq 0$, which means the FONCDNUP can achieve asymptotical synchronization under the controller. □

3.2. Pinning Synchronization for FOCDNUP

In this subsection, we explore the pinning synchronization of the following fractional-order complex dynamical networks with uncertain parameters (FOCDNUP): the drive system is described as

$${}_{t_0}^{c}D_t^{\alpha}\tilde{\varpi}_i(t)=(D+\Delta D(t))\tilde{\varpi}_i(t)+(Q+\Delta Q(t))g(\tilde{\varpi}_i(t))+c\sum_{j=1}^{N}d_{ij}\Lambda\tilde{\varpi}_j(t), \tag{18}$$

and the response system is described as

$$ {}_{t_0}^{c}D_t^{\alpha}\tilde{s}_i(t) = (D+\Delta D(t))\tilde{s}_i(t) + (Q+\Delta Q(t))g(\tilde{s}_i(t)) + c\sum_{j=1}^{N} d_{ij}\Lambda\tilde{s}_j(t) + \tilde{u}_i(t), \tag{19} $$

where $0 < \alpha < 1$, $i = 1, 2, \cdots, n$, $\tilde{\omega}_i(t)$ and $\tilde{s}_i(t)$ are the state of the i-node, D and is the real constant matrix, and Q indicate the weight matrix. $g(\tilde{\omega}_i(t))$ and $g(\tilde{s}_i(t))$ show the continuous nonlinear functions. $\tilde{\Lambda} = \mathrm{diag}(\tilde{\varepsilon_1}, \tilde{\varepsilon_2}, \cdots, \tilde{\varepsilon_n}) > 0$ is the internal coupling matrix of the networks. $(\tilde{d_{ij}})_{n\times n}$ is the outer coupling matrix, and if they have a linkage in the node i to j, $\tilde{d_{ij}} \neq 0$; otherwise, $\tilde{d_{ij}} = 0$. $\Delta D(t)$ and $\Delta Q(t)$ are the parametric uncertainties.

The sync-error vector is defined as

$$ \hat{e}_i(t) = \tilde{s}_i(t) - \tilde{\omega}_i(t). \tag{20} $$

Based on (18) and (19), the sync-error system is expressed as

$$ {}_{t0}^{c}D_t^{\alpha}\hat{e}_i(t) = (D+\Delta D(t))\hat{e}_i(t) + (Q+\Delta Q(t))g(\hat{e}_i(t)) + \tilde{c}\sum_{j=1}^{N} \tilde{d}_{ij}\tilde{\Lambda}\hat{e}_i(t) + \tilde{u}_i(t). \tag{21} $$

Then, the pinning controller of FOCDNUP is described as

$$ \tilde{u}_i(t) = \begin{cases} -\tilde{\delta}_i\hat{e}_i(t), & i = 1, 2, \cdots, m \\ 0, & i = m+1, m+2, \cdots, n. \end{cases} \tag{22} $$

Synchronizing the FOCDNUP by the pinning controller is the next task.

Theorem 2. *Under Assumptions 1 and 2, and scalar $0 < \alpha < 1$, the FOCDNUP can achieve synchronization under the pinning controller, if the following inequalities hold:*

$$ D + \frac{1}{2}M_dM_d^{\top} + \frac{1}{2}H_d^{\top}H_d + LQ + \frac{1}{2}LM_qM_q^{\top} + \frac{1}{2}LH_q^{\top}H_q + \tilde{c}\sum_{j=1}^{N}\tilde{d}_{ij}\tilde{\Lambda} - \sum_{i=1}^{m}\tilde{\delta}_i < 0. $$

Proof. Construct the following Lyapunov function:

$$ V(t) = \sum_{i=1}^{n}|\hat{e}_i(t)|, \tag{23} $$

then, taking the fractional derivative of $V(t)$ by Lemma 1, one can obtain

$$ \begin{aligned} {}_{t_0}^{c}D_t^{\alpha}V(t) =& {}_{t_0}^{c}D_t^{\alpha}\sum_{i=1}^{n}|\hat{e}_i(t)| \\ \leq& \sum_{i=1}^{n}\mathrm{sign}^{\top}(\hat{e}_i(t)) {}_{t_0}^{c}D_t^{\alpha}\hat{e}_i(t) \\ \leq& \sum_{i=1}^{n}\mathrm{sign}^{\top}(\hat{e}_i(t))[(D+\Delta D(t))\hat{e}_i(t) + (Q+\Delta Q(t))g(\hat{e}_i(t)) \\ &+ c\sum_{j=1}^{N}\tilde{d}_{ij}\tilde{\Lambda}\hat{e}_i(t) + \tilde{u}_i(t)] \\ \leq& \sum_{i=1}^{n}\mathrm{sign}^{\top}(\hat{e}_i(t))(D+\Delta D(t))\hat{e}_i(t) \\ &+ \sum_{i=1}^{n}\mathrm{sign}^{\top}(\hat{e}_i(t))(Q+\Delta Q(t))g(\hat{e}_i(t)) \\ &+ \sum_{i=1}^{n}\mathrm{sign}^{\top}(\hat{e}_i(t))(\tilde{c}\sum_{j=1}^{N}\tilde{d}_{ij}\tilde{\Lambda}\hat{e}_i(t) + \tilde{u}_i(t)). \end{aligned} \tag{24} $$

It follows from Lemma 2 and Assumption 2 that

$$\begin{aligned} V_1 &= \sum_{i=1}^{n} \operatorname{sign}^{\top}(\hat{e}_i(t))(D + \Delta D(t))\hat{e}_i(t) \\ &\leq \sum_{i=1}^{n} |(D + \Delta D(t))\hat{e}_i(t)| \\ &\leq \sum_{i=1}^{n} |(D + M_d F(t) H_d)\hat{e}_i(t)| \\ &\leq \sum_{i=1}^{n} |D + \frac{1}{2} M_d M_d^{\top} + \frac{1}{2} H_d^{\top} H_d \hat{e}_i(t)|. \end{aligned} \tag{25}$$

Using Assumption 1, one obtains

$$\begin{aligned} V_2 &= \sum_{i=1}^{n} \operatorname{sign}^{\top}(\hat{e}_i(t))(Q + \Delta Q(t))g(\hat{e}_i(t)) \\ &\leq \sum_{i=1}^{n} |Q + \Delta Q(t))L\hat{e}_i(t)| \\ &\leq \sum_{i=1}^{n} |(Q + M_q F(t) H_q)L\hat{e}_i(t)| \\ &\leq \sum_{i=1}^{n} |(Q + \frac{1}{2} M_q M_q^{\top} + \frac{1}{2} H_q^{\top} H_q)L\hat{e}_i(t)|. \end{aligned} \tag{26}$$

Adding the pinning controller $\tilde{u}_i(t)$ to (24), one has

$$\begin{aligned} V_3 &= \sum_{i=1}^{n} \operatorname{sign}^{\top}(\hat{e}_i(t))(\tilde{c} \sum_{j=1}^{N} d_{ij} \tilde{\Lambda} \hat{e}_i(t) + \tilde{u}_i(t)) \\ &\leq \sum_{i=1}^{n} |\tilde{c} \sum_{j=1}^{N} \tilde{d}_{ij} \tilde{\Lambda} \hat{e}_i(t)| - \sum_{i=1}^{m} \tilde{\delta}_i |\hat{e}_i(t)|. \end{aligned} \tag{27}$$

By adding (25)–(27) to (24), we have

$$\begin{aligned} {}_{t_0}^{c}D_t^{\alpha} V(t) =& V_1 + V_2 + V_3 \\ \leq& \sum_{i=1}^{n} |D + \frac{1}{2} M_d M_d^{\top} + \frac{1}{2} H_d^{\top} H_d \hat{e}_i(t) + \tilde{c} \sum_{j=1}^{N} \tilde{d}_{ij} \tilde{\Lambda} \hat{e}_i(t) - \tilde{\delta}_i \hat{e}_i(t) \\ &+ (Q + \frac{1}{2} M_q M_q^{\top} + \frac{1}{2} H_q^{\top} H_q) L\hat{e}_i(t)| \\ \leq& \sum_{i=1}^{n} [D + \frac{1}{2} M_d M_d^{\top} + \frac{1}{2} H_d^{\top} H_d + LQ + \frac{1}{2} L M_q M_q^{\top} \\ &+ \frac{1}{2} L H_q^{\top} H_q + \tilde{c} \sum_{j=1}^{N} \tilde{d}_{ij} \tilde{\Lambda} - \sum_{i=1}^{m} \tilde{\delta}_i] |\hat{e}_i(t)|. \end{aligned} \tag{28}$$

If $D + \frac{1}{2} M_d M_d^{\top} + \frac{1}{2} H_d^{\top} H_d + LQ + \frac{1}{2} L M_q M_q^{\top} + \frac{1}{2} L H_q^{\top} H_q + \tilde{c} \sum_{j=1}^{N} \tilde{d}_{ij} \tilde{\Lambda} - \sum_{i=1}^{m} \tilde{\delta}_i < 0$, the FOCDNUP is pinning synchronization under the controller. □

4. Numerical Simulation

In this section, the viability and validity of the approaches are verified by two numerical instances.

Example 1. *Suppose that the below FONCDNUP is made up of n nodes and it is given in the following way:*

$$ {}_{t_0}^{c}D_t^{\alpha}\varpi_i(t) = A_0\varpi_i(t) + B_0\hbar(\varpi_i(t)) + c\sum_{j=1}^{N} d_{ij}\Lambda\varpi_j(t), \tag{29} $$

and

$$ {}_{t_0}^{c}D_t^{\alpha}s_i(t) = (E_0 + \Delta E(t))s_i(t) + (G_0 + \Delta G(t))\hbar(s_i(t)) + c\sum_{j=1}^{N} d_{ij}\Lambda s_j(t) + u_i(t). \tag{30} $$

The controller is

$$ u_i(t) = -(E_0 + \Delta E(t) - A_0)\varpi_i(t) - (G_0 + \Delta G(t))\hbar(\varpi_i(t)) + B_0\hbar(\varpi_i(t) - \delta_i e_i(t). \tag{31} $$

Considering the 10 nodes of FONCDNUP, where $\delta = 20$, $\varpi_i(t) = [\varpi_{i1}, \varpi_{i2}, \varpi_{i3}, \varpi_{i4}]^\top$, $s_i(t) = [s_{i1}, s_{i2}, s_{i3}, s_{i4}]^\top$, $i = 1, 2, \cdots, 10$, c is the coupling coefficient, which represents the degree of connection between each node, and $c = 0.01$, $a = 0.25, b = 8.1$; and the nonlinear functions can be expressed $\hbar(\varpi_i(t)) = [a * \tanh(\varpi_{i1}(t)), a * \tanh(\varpi_{i2}(t)), a * \tanh(\varpi_{i3}(t)), a * \tanh(\varpi_{i4}(t))]^\top$; $\hbar(s_i(t)) = [b * \tanh(s_{i1}(t)), b * \tanh(s_{i2}(t)), b * \tanh(s_{i3}(t)), b * \tanh(s_{i4}(t))]^\top$.

The weight matrices and the parametric matrices are

$$ A_0 = \begin{pmatrix} -18.058 & 0 & 0 & 0 \\ 0 & -1.256 & 0 & 0 \\ 0 & 0 & -10.847 & 0 \\ 0 & 0 & 0 & -1.865 \end{pmatrix}, \quad B_0 = \begin{pmatrix} 10.8 & 0 & 5.5 & 0.18 \\ 0 & -1.55 & 0.01 & 0.05 \\ 15.3 & 1 & -10 & 0 \\ 2.5 & 0 & 0 & -2.815 \end{pmatrix}. $$

$$ E_0 = \begin{pmatrix} -20.204 & 0 & 0 & 0 \\ 0 & -4.15 & 0 & 0 \\ 0 & 0 & -5.357 & 0 \\ 0 & 0 & 0 & -1.613 \end{pmatrix}, \quad G_0 = \begin{pmatrix} -1.048 & 0.015 & 0.05 & 0.6 \\ -0.01 & 0.85 & 0 & 1.47 \\ 0 & -1.3 & -4.25 & -1.45 \\ 0.86 & 0 & 3 & -1.45 \end{pmatrix}. $$

The internal coupling matrix can be shown as

$$ \Lambda = \begin{pmatrix} 0.25 & 0 & 0 & 0 \\ 0 & 0.25 & 0 & 0 \\ 0 & 0 & 0.25 & 0 \\ 0 & 0 & 0 & 0.25 \end{pmatrix}. $$

The outer coupling matrix can be indicated by

$$ (d_{ij})_{n\times n} = \begin{pmatrix} -2.1 & 0 & 1.15 & 0 & 2.05 & -2 & 1.02 & -1 & 0.22 & -2.15 \\ -2.1 & -1.15 & 0 & -0.12 & 0.21 & -0.45 & 0 & 1.5 & 0.1 & -3.3 \\ 0 & -1 & -3.1 & 0 & 1 & -1.5 & 0 & -1.25 & -1.15 & 1.02 \\ 2.5 & 0 & 1.5 & -2.2 & 1.5 & 0 & -1.5 & 0 & -2.03 & 0.5 \\ 0 & -1 & 0 & 1 & -2.35 & -1.25 & -1.5 & 3.01 & 0.5 & -1.1 \\ -1.01 & 0 & 2 & -2.1 & 1.05 & -1.5 & 0 & 0.1 & -1 & 0 \\ 0.5 & 0 & -1 & 2.1 & 0 & 1.5 & -1.5 & -0.5 & 1.01 & 1.45 \\ -2.03 & 0.1 & -1.01 & 1.2 & -1.5 & 0 & -1.2 & -1.25 & 2.35 & -0.2 \\ 1 & -2.51 & 0 & 1.5 & -1 & 0.2 & 0.5 & 1.06 & -1.15 & -1.25 \\ 1.5 & -3.13 & 0.5 & -0.5 & 0 & -1.15 & 3 & 0 & 0.2 & -1 \end{pmatrix}. $$

The parameter uncertainties matrices can be shown in terms of

$$M_e = \begin{pmatrix} 0.1 & 0 & 0 & 0 \\ 0 & 0.5 & 0 & 0 \\ 0 & 0 & 0.2 & 0 \\ 0 & 0 & 0 & 0.3 \end{pmatrix}, \quad H_e = \begin{pmatrix} 0.2 & 0 & 0 & 0 \\ 0 & 0.1 & 0 & 0 \\ 0 & 0 & 0.2 & 0 \\ 0 & 0 & 0 & 0.5 \end{pmatrix},$$

$$F_e(t) = \begin{pmatrix} \cos(\varpi_1(t)) & 0 & 0 & 0 \\ 0 & \cos(\varpi_2(t)) & 0 & 0 \\ 0 & 0 & \cos(\varpi_3(t)) & 0 \\ 0 & 0 & 0 & \cos(\varpi_4(t)) \end{pmatrix},$$

and

$$M_g = \begin{pmatrix} 1 & 0 & 0 & 0 \\ 0 & 0.9 & 0 & 0 \\ 0 & 0 & 1 & 0 \\ 0 & 0 & 0 & 0.3 \end{pmatrix}, \quad H_g = \begin{pmatrix} 1 & 0 & 0 & 0 \\ 0 & 0.9 & 0 & 0 \\ 0 & 0 & 0.8 & 0 \\ 0 & 0 & 0 & 1 \end{pmatrix},$$

$$F_g(t) = \begin{pmatrix} 0.41\cos(s_1(t)) & 0 & 0 & 0 \\ 0 & \cos(s_2(t)) & 0 & 0 \\ 0 & 0 & 0.3\cos(s_3(t)) & 0 \\ 0 & 0 & 0 & 0.13\cos(s_4(t)) \end{pmatrix}.$$

We choose the appropriate initial values. Then, using the MATLAB R2020a, the Admas–Bashforth–Moulton predictor corrector method is employed for numerical simulation. If the previous parameter matrix changes, it will extend our control time. Figures 1–4 show the trajectories of sync−error (9) (e_{i1}, e_{i2}, e_{i3}, e_{i4}) without control, respectively. We can observe that the (29) and the (30) without control is unsynchronized. Figures 5–8 reflect the trajectories of sync−error 9 (e_{i1}, e_{i2}, e_{i3}, e_{i4}) under control, respectively. Figure 9 shows the trajectories of total sync−error systems (9) not under control. Figure 10 shows the trajectories of total sync−error systems (9) under the control. From the simulation results and graphs, it can be obtained that the error system is actuated to the point of initial. Clearly, (29) and (30) can achieve asymptotic synchronization. This shows the effectiveness and feasibility of Theorem 1.

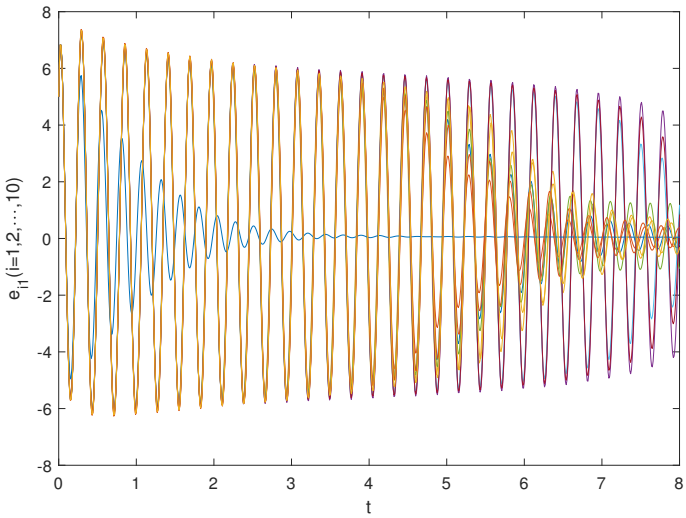

Figure 1. Time behaviors of sync−error trajectories $e_{i1}(i = 1, 2, \cdots, 10)$ without controller.

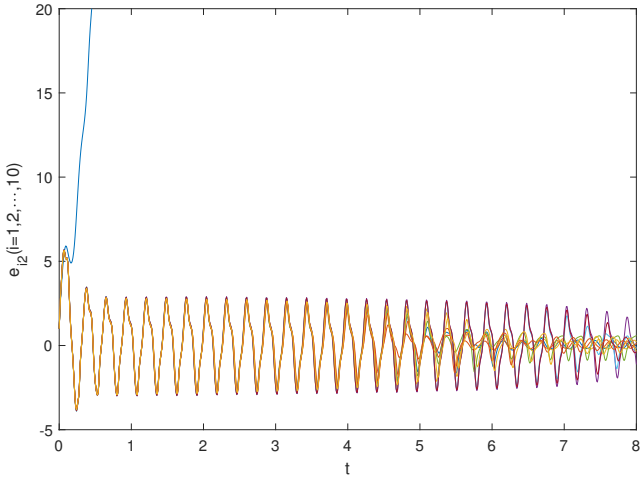

Figure 2. Time behaviors of sync−error trajectories $e_{i2}(i = 1, 2, \cdots, 10)$ without controller.

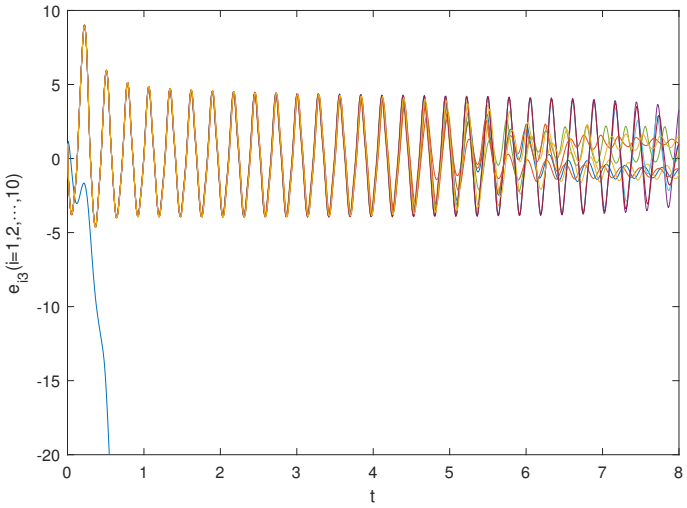

Figure 3. Time behaviors of sync−error trajectories $e_{i3}(i = 1, 2, \cdots, 10)$ without controller.

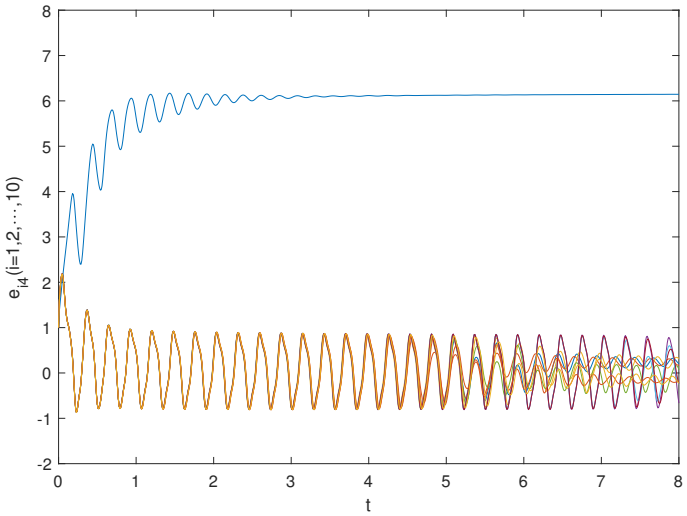

Figure 4. Time behaviors of sync−error trajectories $e_{i4}(i = 1, 2, \cdots, 10)$ without controller.

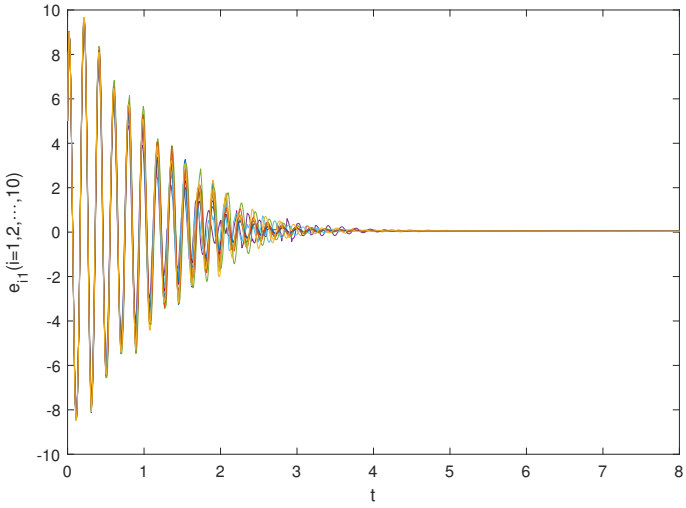

Figure 5. Time behaviors of sync−error trajectories $e_{i1}(i = 1, 2, \cdots, 10)$ with controller.

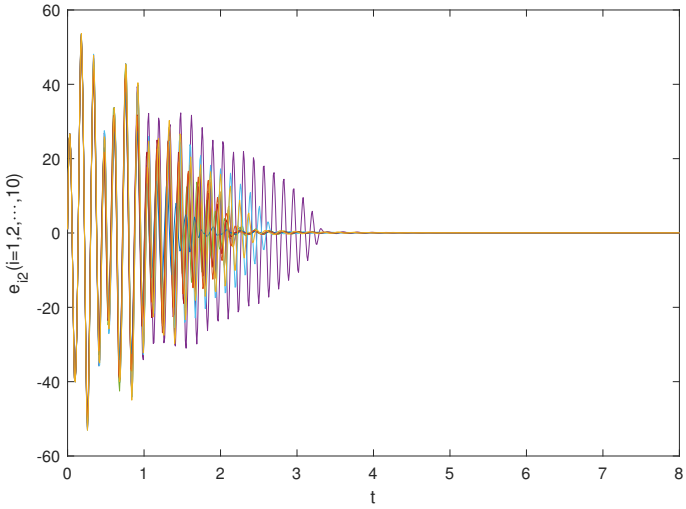

Figure 6. Time behaviors of sync−error trajectories $e_{i2}(i = 1, 2, \cdots, 10)$ with controller.

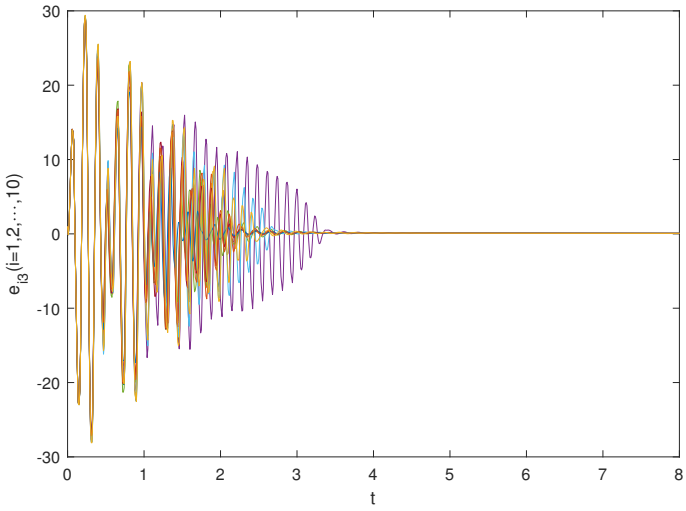

Figure 7. Time behaviors of sync−error trajectories $e_{i3}(i = 1, 2, \cdots, 10)$ with controller.

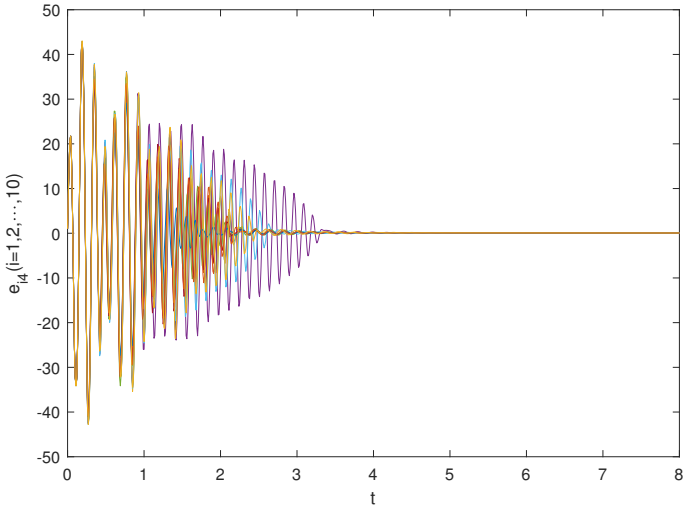

Figure 8. Time behaviors of sync−error trajectories $e_{i4}(i = 1, 2, \cdots, 10)$ with controller.

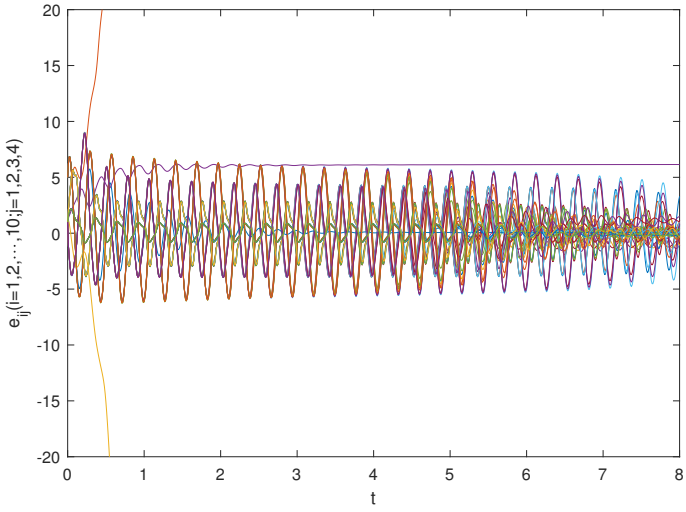

Figure 9. Time behaviors of sync−error trajectories $e_{ij}(i = 1, 2, \cdots, 10; j = 1, 2, 3, 4)$ without controller.

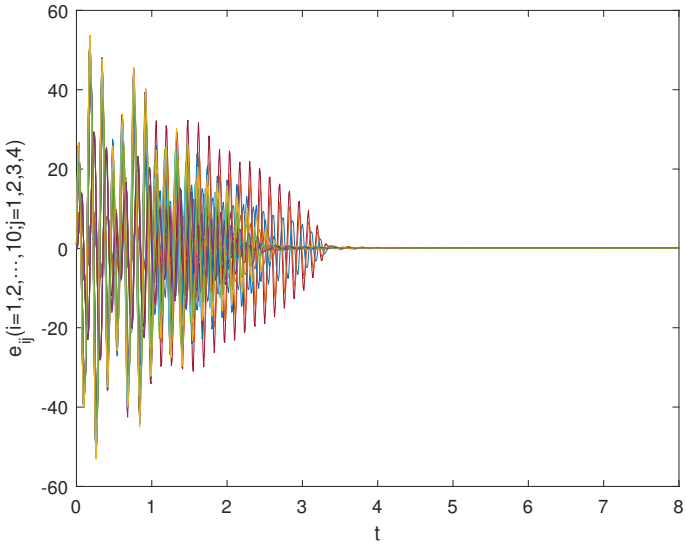

Figure 10. Time behaviors of sync−error trajectories $e_{ij}(i = 1, 2, \cdots, 10; j = 1, 2, 3, 4)$ with controller.

Example 2. *Supposed that the below FOCDNUP is made up of n nodes and it is given in the following way:*

$$ {}_{t_0}^{c}D_t^{\alpha}\tilde{\omega}_i(t) = (D + \Delta D(t))\tilde{\omega}_i(t) + (Q + \Delta B(t))g(\tilde{\omega}_i(t)) + \tilde{c}\sum_{j=1}^{N}\tilde{d}_{ij}\tilde{\Lambda}\tilde{x}_j(t), \tag{32} $$

and

$$ {}_{t_0}^{c}D_t^{\alpha}\tilde{s}_i(t) = (D_0 + \Delta D(t))\tilde{s}_i(t) + (Q + \Delta Q(t))g(\tilde{s}_i(t)) + \tilde{c}\sum_{j=1}^{N}\tilde{d}_{ij}\tilde{\Lambda}\tilde{y}_j(t) + \tilde{u}_i(t). \tag{33} $$

The 10 nodes of FOCDNUP are considered, where $\delta = 15$, $\tilde{\omega}_i(t) = [\tilde{\omega}_{i1}, \tilde{\omega}_{i2}, \tilde{\omega}_{i3}, \tilde{\omega}_{i4}]^{\top}$, $\tilde{s}_i(t) = [\tilde{s}_{i1}, \tilde{s}_{i2}, \tilde{s}_{i3}, \tilde{s}_{i4},]^{\top}$ $i = 1, 2, \cdots, 10$, $c = 5$, $\hat{a} = 0.01$, $\hat{b} = 0.01$; and the nonlinear functions can be expressed as: $g(\tilde{\omega}_i(t)) = [\hat{a} * \tanh(\tilde{\omega}_{i1}(t)), \hat{a} * \tanh(\tilde{\omega}_{i2}(t)), \hat{a} * \tanh(\tilde{\omega}_{i3}(t)), \hat{a} * \tanh(\tilde{\omega}_{i4}(t))]^{\top}$; $g(\tilde{s}_i(t)) = [\hat{b} * \tanh(\tilde{s}_{i1}(t)), \hat{b} * \tanh(\tilde{s}_{i2}(t)), \hat{b} * \tanh(\tilde{s}_{i3}(t)), \hat{b} * \tanh(\tilde{s}_{i4}(t))]^{\top}$.

The first five nodes are added to the controller, namely,

$$ \tilde{u}_i(t) = \begin{cases} -15\hat{e}_i(t), & i = 1, 2, 3, 4, 5 \\ 0, & i = 6, 7, 8, 9, 10. \end{cases} \tag{34} $$

The weight matrices and parametric matrices are

$$ D = \begin{pmatrix} -3.54 & 0 & 0 & 0 \\ 0 & -2.96 & 0 & 0 \\ 0 & 0 & -5.07 & 0 \\ 0 & 0 & 0 & -2.93 \end{pmatrix}, \quad Q = \begin{pmatrix} -15.5 & 0.05 & 5.1 & 0 \\ 70 & 0 & -15.01 & 35 \\ 60.1 & -10.1 & -8.25 & 15.5 \\ -0.1 & -0.03 & 30.01 & -0.35 \end{pmatrix}. $$

And the inner coupling matrices can be expressed in terms of

$$ \tilde{\Lambda} = \begin{pmatrix} 0.25 & 0 & 0 & 0 \\ 0 & 0.25 & 0 & 0 \\ 0 & 0 & 0.25 & 0 \\ 0 & 0 & 0 & 0.25 \end{pmatrix}. $$

The outer coupling matrix can be indicated by

$$ (\tilde{d_{ij}})_{n\times n} = \begin{pmatrix} -2 & 1 & 0 & 1 & 0 & 0 & 0 & 0 & 0 & 0 \\ 0 & -2 & 1 & 0 & 1 & 0 & 0 & 0 & 0 & 0 \\ 1 & 0 & -3 & 0 & 0 & 1 & 1 & 0 & 0 & 0 \\ 0 & 0 & 1 & -1 & 0 & 0 & 0 & 0 & 0 & 0 \\ 0 & 1 & 0 & 1 & -3 & 0 & 0 & 0 & 1 & 0 \\ 1 & 0 & 0 & 0 & 0 & -1 & 0 & 0 & 0 & 0 \\ 0 & 1 & 0 & 0 & 0 & 0 & -1 & 0 & 0 & 0 \\ 1 & 1 & 0 & 0 & 0 & 0 & 0 & -2 & 0 & 0 \\ 1 & 0 & 1 & 0 & 0 & 0 & 0 & 0 & -2 & 0 \\ 0 & 0 & 1 & 0 & 0 & 0 & 0 & 0 & 0 & -1 \end{pmatrix}. $$

The matrices of parameter uncertainties are

$$M_d = \begin{pmatrix} 1 & 0 & 0 & 0 \\ 0 & 0.81 & 0 & 0 \\ 0 & 0 & 1 & 0 \\ 0 & 0 & 0 & 1 \end{pmatrix}, \quad H_d = \begin{pmatrix} 1 & 0 & 0 & 0 \\ 0 & 1 & 0 & 0 \\ 0 & 0 & 0.8 & 0 \\ 0 & 0 & 0 & 0.3 \end{pmatrix},$$

$$F_d(t) = \begin{pmatrix} 0.41\cos(\tilde{\omega}_1(t)) & 0 & 0 & 0 \\ 0 & \cos(\tilde{\omega}_2(t)) & 0 & 0 \\ 0 & 0 & 0.3\cos(\tilde{\omega}_3(t)) & 0 \\ 0 & 0 & 0 & 0.13\cos(\tilde{\omega}_4(t)) \end{pmatrix},$$

and

$$M_q = \begin{pmatrix} 0.1 & 0 & 0 & 0 \\ 0 & 0.5 & 0 & 0 \\ 0 & 0 & 0.2 & 0 \\ 0 & 0 & 0 & 0.15 \end{pmatrix}, \quad H_q = \begin{pmatrix} 0.2 & 0 & 0 & 0 \\ 0 & 0.1 & 0 & 0 \\ 0 & 0 & 0.2 & 0 \\ 0 & 0 & 0 & 1 \end{pmatrix},$$

$$F_q(t) = \begin{pmatrix} \cos(\tilde{s}_1(t)) & 0 & 0 & 0 \\ 0 & \cos(\tilde{s}_2(t)) & 0 & 0 \\ 0 & 0 & \cos(\tilde{s}_3(t)) & 0 \\ 0 & 0 & 0 & \cos(\tilde{s}_4(t)) \end{pmatrix}.$$

We choose the appropriate initial values and use the same MATLAB and methods as in Example 1. Figures 11–14 show the trajectories of sync−error (20) ($\hat{e}_{i1}$, $\hat{e}_{i2}$, $\hat{e}_{i3}$, $\hat{e}_{i4}$) not under control, respectively. We can observe that (32) and (33) not under control are unsynchronized. Figures 15–18 reflect the trajectories of sync−error (20) ($\hat{e}_{i1}$, $\hat{e}_{i2}$, $\hat{e}_{i3}$, $\hat{e}_{i4}$) under control, respectively. Figure 19 shows the trajectories of total sync−error systems (20) not under control. Figure 20 shows the trajectories of total sync−error systems (20) under the control. From the simulation results and graphs, it can be obtained that the error system is actuated to the point of initial; it is clear that (32) and (33) can achieve asymptotic synchronization. This shows the effectiveness and feasibility of Theorem 2.

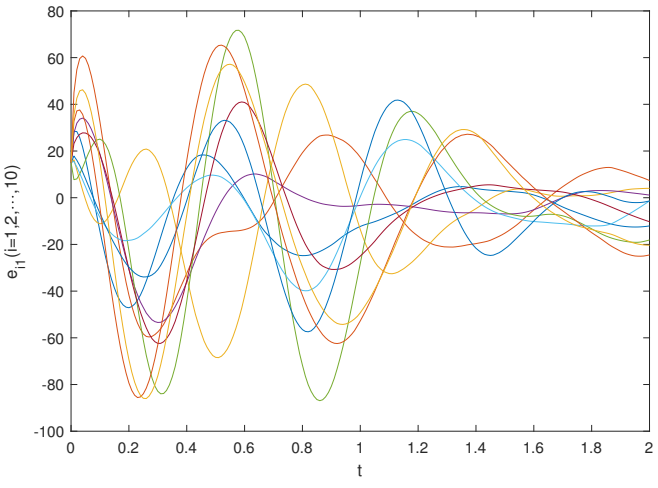

Figure 11. Time behaviors of pinning sync−error trajectories $\hat{e}_{i1}(i = 1, 2, \cdots, 10)$ without controller.

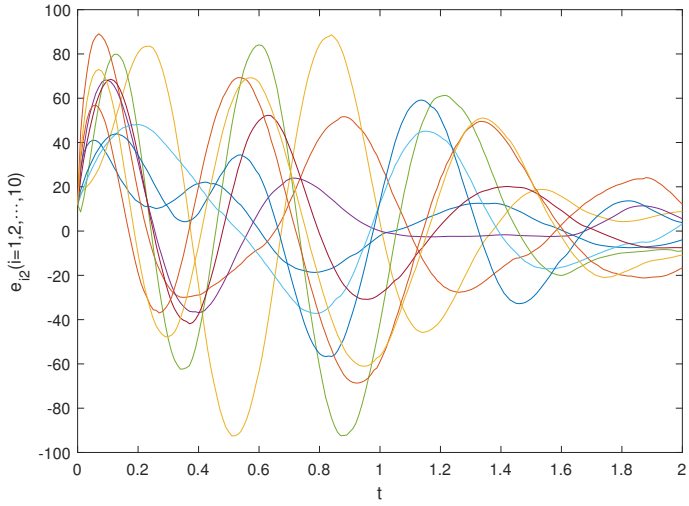

Figure 12. Time behaviors of pinning sync−error trajectories $\hat{e}_{i2}(i = 1, 2, \cdots, 10)$ without controller.

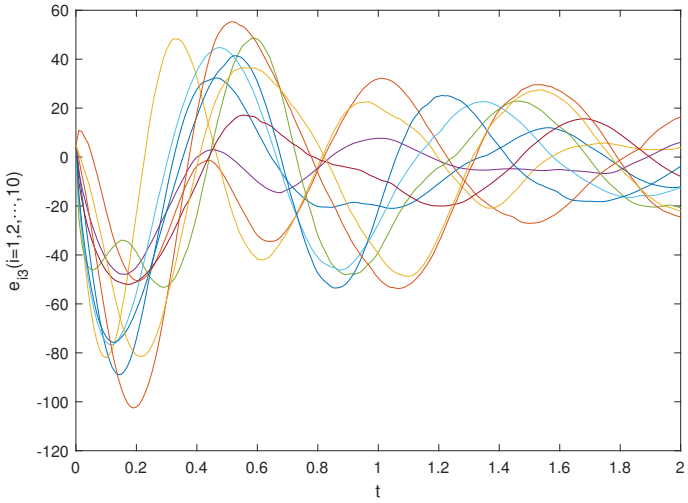

Figure 13. Time behaviors of pinning sync−error trajectories $\hat{e}_{i3}(i = 1, 2, \cdots, 10)$ without controller.

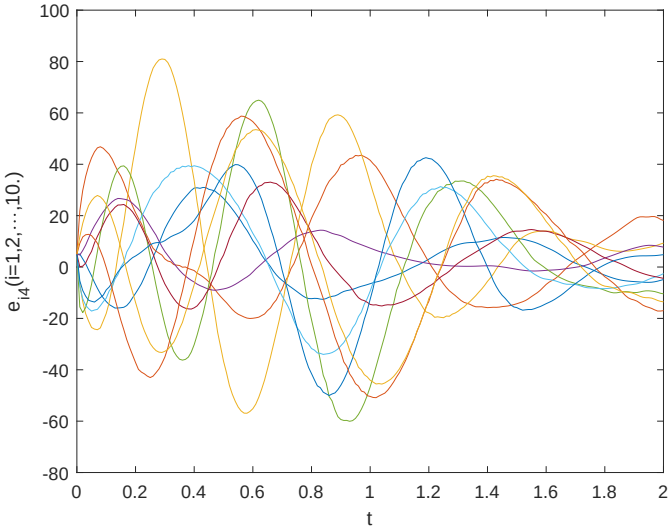

Figure 14. Time behaviors of pinning sync−error trajectories $\hat{e}_{i4}(i = 1, 2, \cdots, 10)$ without controller.

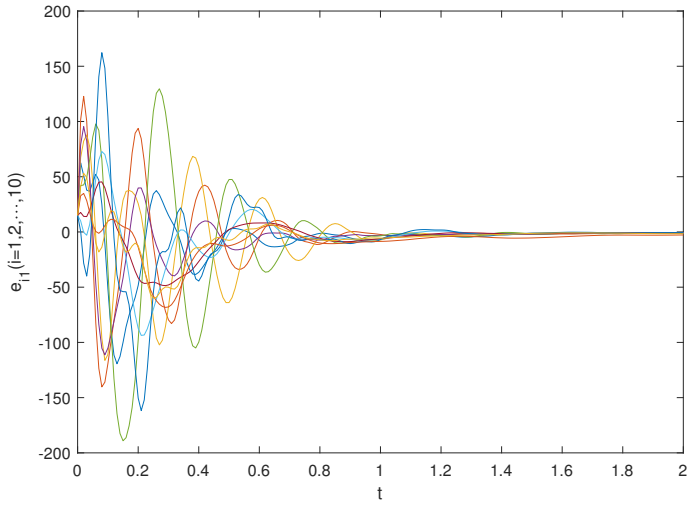

Figure 15. Time behaviors of pinning sync−error trajectories $\hat{e}_{i1}(i = 1, 2, \cdots, 10)$ with controller.

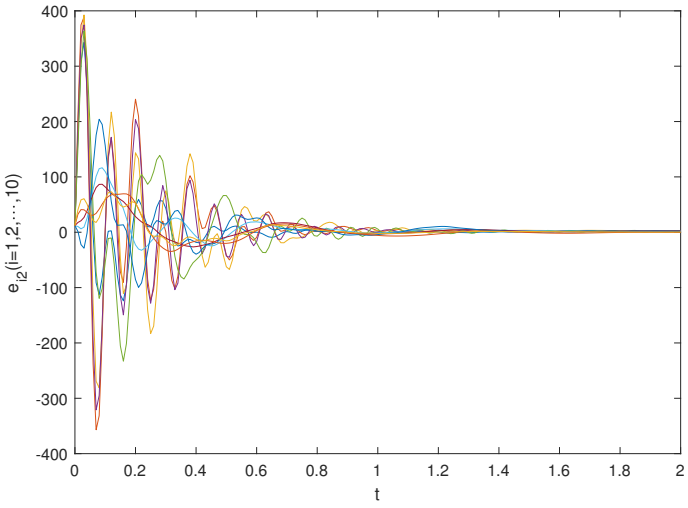

Figure 16. Time behaviors of pinning sync−error trajectories $\hat{e}_{i2}(i = 1, 2, \cdots, 10)$ with controller.

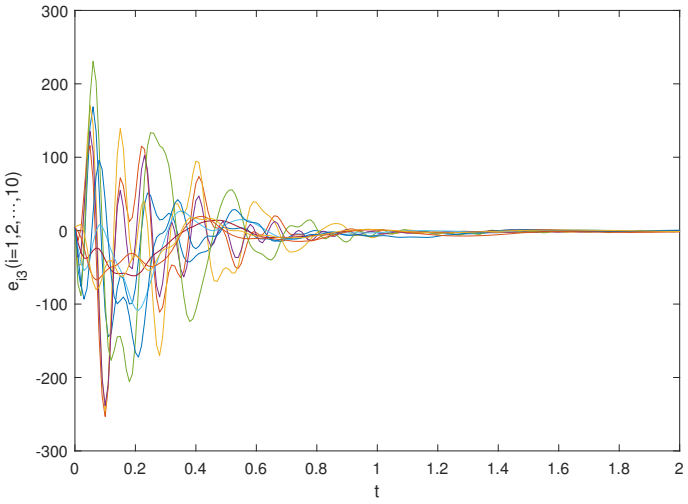

Figure 17. Time behaviors of pinning sync−error trajectories $\hat{e}_{i3}(i = 1, 2, \cdots, 10)$ with controller.

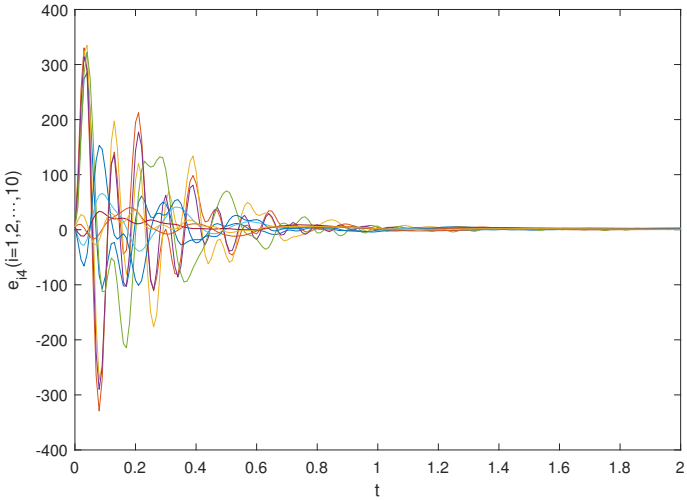

Figure 18. Time behaviors of pinning sync−error trajectories $\hat{e}_{i4}(i = 1, 2, \cdots, 10)$ with controller.

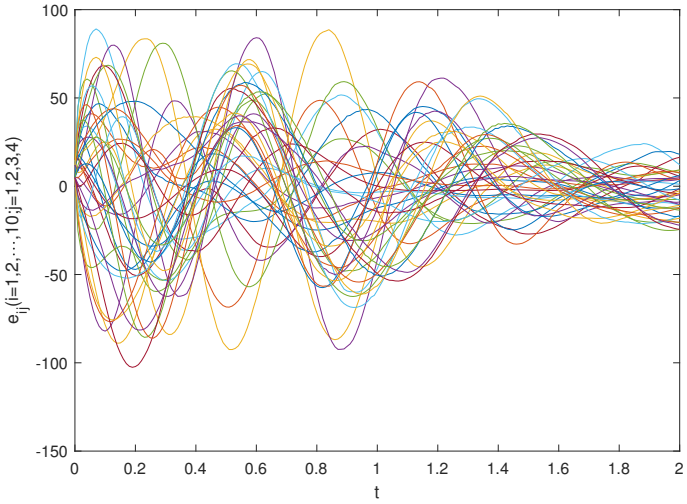

Figure 19. Time behaviors of pinning sync−error trajectories $\hat{e}_{ij}(i = 1, 2, \cdots, 10; j = 1, 2, 3, 4)$ without controller.

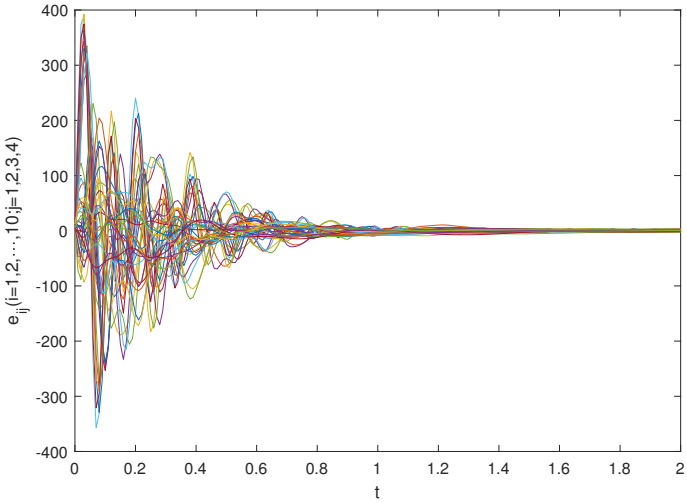

Figure 20. Time behaviors of pinning sync−error trajectories $\hat{e}_{ij}(i = 1, 2, \cdots, 10; j = 1, 2, 3, 4)$ with controller.

5. Conclusions

The asymptotic synchronization of FONCDNUP was studied via a novel control. Several sufficient conditions were derived for ensuring the asymptotic synchronization of FONCDNUP, utilizing fractional differential theory, differential inclusion theory, and the Lyapunov method. The pinning synchronization of FOCDNUP was investigated, where Parameter uncertainties were introduced to the networks. Instead of adding controllers to all nodes, controllers were only added to the first five nodes, reducing costs and enhancing efficiency. Finally, two numerical instances were also presented to demonstrate the effectiveness of the proposed approaches. However, this paper does not consider time delays or extending pinning control to fractional nonidentical complex networks. In the future, the inclusion of time-varying delays in FONCDNUP will be considered, along with the exploration of pinning control for non-identical networks, which presents an interesting and challenging area.

Author Contributions: Y.W. proposed the main the idea and prepared the manuscript initially. X.H. gave the numerical simulation of this paper. T.L. revised the English grammar of this paper. All authors have read and agreed to the published version of the manuscript.

Funding: This work is partly funded by Sichuan University of Science and Engineering (Grant No. 2022RC12) and the Postgraduate Innovation Fund Project of Sichuan University of Science and Engineering (Grant No. Y2022191).

Institutional Review Board Statement: Not applicable.

Informed Consent Statement: Not applicable.

Data Availability Statement: The data used to support the findings of this study are available from the corresponding author upon request.

Conflicts of Interest: The authors declare no conflict of interest.

References

1. Fan, Y.; Huang, X.; Wang, Z.; Li, Y. Nonlinear dynamics and chaos in a simplified memristor-based fractional-order neural network with discontinuous memductance function. *Nonlinear Dyn.* **2018**, *93*, 611–627. [CrossRef]
2. Rajivganthi, C.; Rihan, F.A.; Lakshmanan, S. Dissipativity analysis of complex-valued BAM neural networks with time delay. *Neural Comput. Appl.* **2019**, *31*, 127–137. [CrossRef]
3. Song, Q.; Shu, H.; Zhao, Z.; Liu, Y.; Alsaadi Fuad, E. Lagrange stability analysis for complex-valued neural networks with leakage delay and mixed time-varying delays. *Neurocomputing* **2017**, *244*, 33–41. [CrossRef]
4. Cao, J.; Guerrini, L.; Cheng, Z. Stability and hopf bifurcation of controlled complex networks model with two delays. *Appl. Math. Comput.* **2019**, *343*, 21–29. [CrossRef]
5. Shukla, M.K.; Sharma, B.B. Secure communication and image encryption scheme based on synchronisation of fractional order chaotic systems using backstepping. *Int. J. Simul. Process Model.* **2018**, *13*, 473–485. [CrossRef]
6. Padovan, J.; Guo, Y. General response of viscoelastic systems modelled by fractional operators. *J. Frankl. Inst.* **1988**, *325*, 247–275. [CrossRef]
7. Majidabad, S.S.; Shandiz, H.T.; Hajizadeh, A. Nonlinear fractional-order power system stabilizer for multi-machine power systems based on sliding mode technique. *Int. J. Robust Nonlinear Control* **2015**, *25*, 1548–1568. [CrossRef]
8. Lazarevi, M.P. Finite time stability analysis of PD alpha fractional control of robotic time-delay systems. *Mech. Res. Commun.* **2006**, *33*, 269–279. [CrossRef]
9. Povstenko, Y.Z. Fractional radial heat conduction in an infinite medium with a cylindrical cavity and associated thermal stresses. *Mech. Res. Commun.* **2010**, *37*, 436–440. [CrossRef]
10. Huang, J.; Shen, T. Well-posedness and dynamics of the stochastic fractional magneto-hydrodynamic equations. *Nonlinear Anal.-Theory Methods Appl.* **2016**, *133*, 102–133. [CrossRef]
11. Sarwar, S.; Zahid, M.A.; Iqbal, S. Mathematical study of fractional-order biological population model using optimal homotopy asymptotic method. *Int. J. Biomath.* **2016**, *9*, 17–33. [CrossRef]
12. Tao, B.; Xiao, M.; Sun, Q.; Cao, J. Hopf bifurcation analysis of a delayed fractional-order genetic regulatory network model. *Neurocomputing* **2017**, *275*, 677–686. [CrossRef]
13. Ionescu, C.M.; Machado, J.A.T.; De Keyser, R. Modeling of the lung impedance using a fractional-order ladder network with constant phase elements. *IEEE Trans. Biomed. Circuits Syst.* **2011**, *5*, 83–89. [CrossRef] [PubMed]
14. Teka, W.W.; Upadhyay, R.K.; Mondal, A. Fractional-order leaky integrate-and-fire model with long-term memory and power law dynamics. *Neural Netw.* **2017**, *93*, 110–125. [CrossRef] [PubMed]

15. Kaslik, E.; Radulescu, I.R. Stability and bifurcations in fractional-order gene regulatory networks. *Appl. Math. Comput.* **2022**, *421*, 126916. [CrossRef]
16. Ren, H.; Karimi, H.R.; Lu, R.; Wu, Y. Synchronization of network systems via aperiodic sampled-data control with constant delay and application to unmanned ground vehicles. *IEEE Trans. Ind. Electron.* **2020**, *67*, 4980–4990. [CrossRef]
17. Mislovaty, R.; Klein, E.; Kanter, I.; Kinzel, W. Public channel cryptography by synchronization of neural networks and chaotic maps. *Phys. Rev. Lett.* **2003**, *91*, 118701. [CrossRef]
18. Prakash, M.; Balasubramaniam, P.; Lakshmanan, S. Synchronization of markovian jumping inertial neural networks and its applications in image encryption. *Neural Netw.* **2016**, *83*, 86–93. [CrossRef]
19. Liu, X.; Liu, Y.; Zhou, L. Quasi-synchronization of nonlinear coupled chaotic systems via aperiodically intermittent pinning control. *Neurocomputing* **2016**, *173*, 759–767. [CrossRef]
20. Yang, X.; Li, C.; Song, Q.; Chen, J.; Huang, J. Global Mittag–Leffler stability and synchronization analysis of fractional-order quaternion-valued neural networks with linear threshold neurons. *Neural Netw.* **2018**, *105*, 88–103. [CrossRef]
21. Zhang, L.; Zhong, J.; Lu, J. Intermittent control for finite-time synchronization of fractional-order complex networks. *Neural Netw.* **2021**, *144*, 11–20. [CrossRef] [PubMed]
22. Bao, H.; Park, J.H.; Cao, J. Adaptive synchronization of fractional-order output-coupling neural networks via quantized output control. *IEEE Trans. Neural Netw. Learn. Syst.* **2021**, *32*, 3230–3239. [CrossRef]
23. Liu, P.; Kong, M.; Xu, M.; Sun, J.; Liu, N. Pinning synchronization of coupled fractional-order time-varying delayed neural networks with arbitrary fixed topology. *Neurocomputing* **2020**, *400*, 46–52. [CrossRef]
24. Ding, Z.; Shen, Y. Projective synchronization of nonidentical fractional-order neural networks based on sliding mode controller. *Neural Netw.* **2016**, *76*, 97–105. [CrossRef] [PubMed]
25. Gu, Y.; Yu, Y.; Wang, H. Synchronization for fractional-order time-delayed memristor-based neural networks with parameter uncertainty. *J. Frankl. Inst.* **2016**, *353*, 3657–3684. [CrossRef]
26. Song, Q.; Chen, Y.; Zhao, Z.; Liu, Y.; Alsaadi, F.E. Robust stability of fractional-order quaternion-valued neural networks with neutral delays and parameter uncertainties. *Neurocomputing* **2021**, *420*, 70–81. [CrossRef]
27. Song, S.; Song, X.; Tejado, I. Projective synchronization for two nonidentical time-delayed fractional-order T-S fuzzy neural networks based on mixed H_∞ /passive adaptive sliding mode control. *Int. J. Mach. Learn. Cybern. B* **2019**, *10*, 799–812. [CrossRef]
28. Ding, Z.; Chen, C.; Wen, S.; Li, S.; Wang, L. Lag projective synchronization of nonidentical fractional delayed memristive neural networks. *Neurocomputing* **2022**, *469*, 138–150. [CrossRef]
29. Chen, J.; Li, C.; Yang, X. Global Mittag–Leffler projective synchronization of nonidentical fractional-order neural networks with delay via sliding mode control. *Neurocomputing* **2018**, *313*, 324–332. [CrossRef]
30. Liang, S.; Wu, R.; Chen, L. Adaptive pinning synchronization in fractional-order uncertain complex dynamical networks with delay. *Phys. A* **2016**, *444*, 49–62. [CrossRef]
31. Wu, X.; Huang, L. Pinning adaptive and exponential synchronization of fractional-order uncertain complex neural networks with time-varying delays. *Neural Process. Lett.* **2019**, *50*, 2373–2388. [CrossRef]
32. Wu, X.; Ai, Q.; Wang, Y. Adaptive and exponential synchronization of uncertain fractional-order t-s fuzzy complex networks with coupling time-varying delays via pinning control strategy. *IEEE Access* **2021**, *9*, 2007–2017. [CrossRef]
33. Podlubny, I. *Fractional Differential Equations*; Academic Press: San Diego, CA, USA, 1999.
34. Zhang, S.; Yu, Y.; Wang, H. Mittag–Leffler stability of fractional-order hopfield neural networks. *Nonlinear Anal.* **2015**, *16*, 104–121. [CrossRef]
35. Xu, S.; Lam, J.; Ho, D.W.; Zou, Y. Global robust exponential stability analysis for interval recurrent neural networks. *Phys. Lett. A* **2004**, *325*, 124–133. [CrossRef]